International Journal of Multidisciplinary Trends

E-ISSN: 2709-9369 P-ISSN: 2709-9350 Impact Factor (RJIF): 6.32 www.multisubjectjournal.com IJMT 2025; 7(10): 47-56

Received: 11-08-2025 Accepted: 13-09-2025

Chol Yong Yun

Faculty of Physical Engineering, Kim Chaek University of Technology, Pyongyang Democratic People's Republic of Korea

In Hak Io

Faculty of Physical Engineering, Kim Chaek University of Technology, Pyongyang Democratic People's Republic of Korea

Yu Gwang Ryu

Faculty of Physical Engineering, Kim Chaek University of Technology, Pyongyang Democratic People's Republic of Korea

Se Chol Pak

Faculty of Electronic Information, Cha Kwang Su University of Education, Sinuiju, Democratic People's Republic of Korea

Chung Hyok Kil

Faculty of Electronic Information, Cha Kwang Su University of Education, Sinuiju, Democratic People's Republic of Korea

U Chol Pak

Hwangnam College of Technology, Pyongyang, Democratic People's Republic of Korea

Corresponding Author: Yu Gwang Ryu Faculty of Physical Engineering, Kim Chaek University of Technology, Pyongyang Democratic People's Republic of Korea

Inverstigation on the lateral force of superconducting magnetic bearing with multi-surface levitation by H- ϕ formulation

Chol Yong Yun, Ju Hak Jo, Yu Gwang Ryu, Se Chol Pak, Chung Hyok Kil and U Chol Pak

DOI: https://www.doi.org/10.22271/multi.2025.v7.i10a.808

Abstract

Advantage of a superconducting magnetic bearing (SMB) is that it is a non-contact and is a self-centering. Thus, it is important procedure to predict the vertical levitation force and the lateral one of SMB. There are a number of efforts to calculate the both direction levitation forces, but the vertical levitation forces are only presented in almost studies. In this contribution, a levitation system composed of a cylindrical high temperature superconducting bulk and a cylindrical permanent magnet is simulated in three dimensional system based on H-φ formulation, and a comparing the results with preceding researches have a good agreement in a vertical and a lateral levitation force. In addition, the three surfaces levitation superconducting magnetic bearing (TSL-SMB) is simulated by the same method, so that the lateral levitation force is predicted under axial load condition. In TSL-SMB without opposite magnetization arrangement, the lateral levitation force in attractive arrangement is larger than ones in repulsive arrangement. In TSL-SMB with opposite magnetization arrangement, the bigger the vertical levitation force, the bigger the lateral ones. This paper will contribute to predict and design the SMB with improvement performance.

Keywords: TSL-SMB, Lateral levitation force, Numerical simulation, H-φ formulation

1. Introduction

In recent years, natural disasters that occur all over the world due to global warming require us to actively protect the ecological environment, minimize the use of fossil fuels and increase the applications of renewable energy more and more. A flywheel energy storage system [1-4] is one of means of using renewable energy, whose capacity mainly depends on built-in bearings (i.e., magnetic bearing or superconducting magnetic bearing (SMB)). Since a SMB has the passive stable levitation, it is very interesting in developing the flywheel system [5, 6]. A number of experimental works were performed to reveal the characteristics and properties of the interaction between a superconductor and a permanent magnet or a magnetic field [7-11]. The modeling of the interaction between superconductor and external magnetic field is a crucial aspect to develop the SMB. It is important to predict and investigate the performance of the SMB without experiment devices, which consumes no few time and resources, there were presented a lot of working results. Among them, the finite element method (FEM) is one of the widely used methods, since the simulation results are reliable and many formulations are employed depending on a different application. The Hformulation is considered to be versatile, widely used for numerical calculation of levitation and magnetization using superconductors. But the disadvantage of H-formulation is that it has a long time to calculate the levitation system, since it is applied to the non-conducting domain. To overcome the disadvantage of H-formulation, the superconducting region and thin coolant region were only considered. In addition, the boundary condition was modeled by analytical formulas such as Biot-Savart law [12-13] and Fourier decomposition [14]. To consider the complex PMs arrangement, a magnetostatic A-formulation finite element model was used [15]. An arbitrary Lagrangian-Eulerian formulation was used to flexibly implement the model of whole region composed of a superconducting bulk and a PM in 2D axisymmetric coordinate system [16-17]. In a SMB, the lateral levitation force is a very important issue to discuss stability, and in a cylindrical levitation system, it can only be predicted by 3D analysis. Accurate prediction of lateral force characteristics in SMB is a prerequisite for improving the rotational stability of the SMB-based devices and for designing a suitable structure of the SMB. A levitation/suspension system composed of a rectangular HTS and a cylindrical PMs was modeled in 3D system so that the magnetic forces were calculated in vertical and the lateral direction displacements [18]. The

characteristics of a SMB such as longitudinal stiffness, transverse stiffness and loss were considered by FEM using the T- Ω formulation [19]. The full 3D finite element calculation, which is essential for predicting the lateral force characteristics, requires a large degree of freedom to increase the computational accuracy due to its own characteristics, and thus, it consumes a long computational time. Alexandre Arsenault et al. proposed H-φ formulation modeling method to provide a crucial solution to further reduce the computational cost of levitation systems consisting of superconductor and PMs [20]. Different Halbach schemes of rotor with PMs in a SMB were considered by 3D H-φ formulation [21]. In this paper, we considered the levitation system composed of a cylindrical HTS bulk and a cylindrical PM based on 3D H-p formulation, and made the implementation of validation by comparing with the results of [13]. In addition, we also considered the TSL-SMB so that we validated the vertical levitation force by comparing 3D H-φ formulation results with 2D axisymmetric H formulation [17, 22] and 2D axisymmetric H-\phi formulation, obtained the lateral levitation forces depending on lateral displacements under axial load condition. Our study is significant in analyzing the performance of flywheel energy storage system using multi-surface levitation superconducting magnetic bearings.

2. H- ϕ Formulation and Validation

2.1. H-φ Formulation

The H- ϕ formulation is implemented by combining the H-formulation in conducting domains with the ϕ -formulation in non-conducting domains, where H, ϕ mean magnetic field and magnetic scalar potential, respectively. The H-formulation is derived from Ampere's and Faraday's laws, which is efficient in modeling the high temperature superconductor. In superconducting regions, the governing H-formulation is expressed as:

$$\nabla \times (\rho \nabla \times \mathbf{H}) = -\mu_0 \frac{\partial \mathbf{H}}{\partial t}$$
(1)

where ρ is the nonlinear resistivity in superconducting cases, and it depends on the external conditions such as a magnetic field and a temperature of coolant, and then μ_0 is the permeability of air.

The resistivity of superconductor is modeled by power law as shown following expression.

$$\rho = \frac{E_c}{J_c(\mathbf{B})} \left(\frac{\|\mathbf{J}\|}{J_c(\mathbf{B})} \right)^{n-1}$$
(2)

where **J** is the current density in superconducting domain, $J_c(B)$ is the critical current density depending on the external magnetic field and temperature, n is the power law exponent, and E_c (= 1 μ V/cm.) is the critical current criterion. $J_c(B)$ can be expressed using Kim model as:

$$J_{c}(\mathbf{B}) = J_{c0} \left(\frac{B_{0}}{B_{0} + |\mathbf{B}|} \right)$$
(3)

where J_{c0} , B_0 are constants depending on a superconducting material.

In non-conducting regions, the magnetic field is expressed from the magnetic scalar potential as:

$$\mathbf{H} = -\nabla \varphi \tag{4}$$

The validity of the applying this definition is mathematically due to the following relation expression.

$$\mathbf{J} = \nabla \times \mathbf{H} = \nabla \times (-\nabla \varphi) = 0 \tag{5}$$

This is good agreement with the physical meaning that the current in the non-conducting region must be zero.

One can derive the equation of the ϕ physics by the divergence-free condition that is expressed as:

$$\nabla \cdot \mathbf{B} = \nabla \cdot (\mu_0 \mathbf{H}) = 0 \tag{6}$$

From equation (6), the equation of the φ physics is expressed as:

$$\nabla \cdot \nabla \varphi = 0 \tag{7}$$

The coupling method between the two physics is presented in appendix of ^[20].

In addition, x, y and z components of the levitation force are calculated as following expressions.

$$\begin{cases} F_x = J_y B_z - J_z B_y \\ F_y = J_z B_x - J_x B_z \\ F_z = J_x B_y - J_y B_x \end{cases}$$
(8)

2.2 Implementation of the H- ϕ formulation and Validation

We performed the implement of the H- ϕ formulation by using the predefined Magnetic Field Formulation (MFH) and Magnetic Field No Currents (MFNC) modules in COMSOL Multiphysics 6.2. In addition, to validate the simulation method, we used the working results of ^[13].

Above mentioned formulations have been already contained in MFH module and MFNC module by thanks to the researchers. The table 1 and Figure 1 show the physical parameters and geometrical model, used in our validation, respectively. In Figure 1, the blue arrow denotes the magnetization direction of PM. The initial positions of PM (i.e., $O_{PM}(x, y, z)$), HTS (i.e., $O_{HTS}(x, y, z)$) are (0, 0, 0) and (0, 0, 25), respectively. The displacement sequence is as following coordinate points, while the moving speed of PM is 1 mm/s.

The moving points of PM = $\{(0,0,25), (0,0,5), (0,7.5,5), (0,-7.5,5), (0,7.5,5), (0,7.5,5), (0,7.5,5)\}$

Table 1: Physical parameters used in our validation.

Symbol	Meaning of symbol	Value	
B_r	PM remanent flux density	1.27T	
E_c	Critical current criterion	$1 \times 10^{-4} \text{ V/m}$	
$J_{ m c0}$	HTS parameter	$2.4 \times 10^8 \mathrm{A/m^2}$	
n	HTS parameter	21	
B_0	HTS parameter	0.37T	
$ ho_{ m air}$	Air resistivity	1 Ω m	
μ_0	Air/HTS permeability	$4\pi \times 10^{-7} \text{ H/m}$	

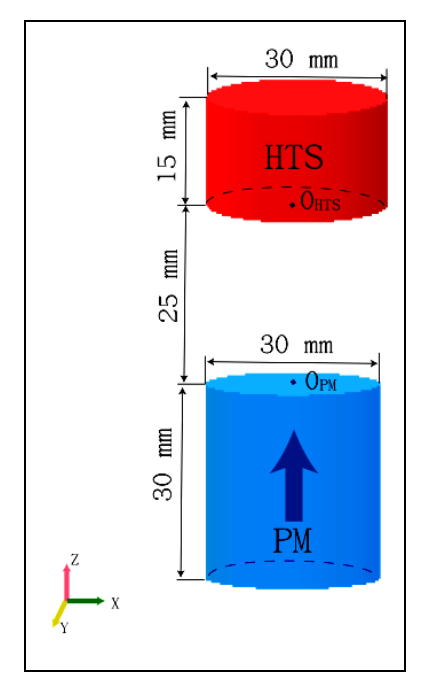
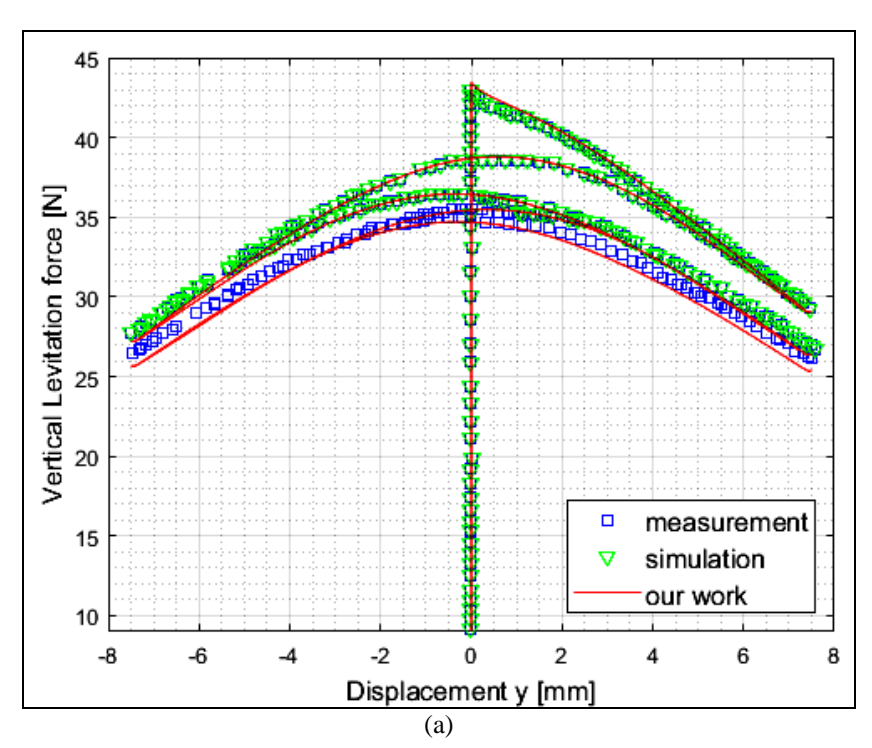


Fig 1: Geometric model used in our validation

The *Moving mesh* (i.e., Laglangian-Eulerian formulations) interface and *Global ODEs and DAEs* interface are adapted to model the relative movement between HTS and PM. The mesh is carried out by free triangle. The maximum size of mesh in HTS domain is 1 mm, the other domains are discretized by coarser.

Figure 2 shows that the results of our validation. The square points with blue color and triangle points with green color denote experimental measurement and simulation data of $^{[13]}$, and then the red curve represents our simulation results calculated by the H- ϕ formulation.



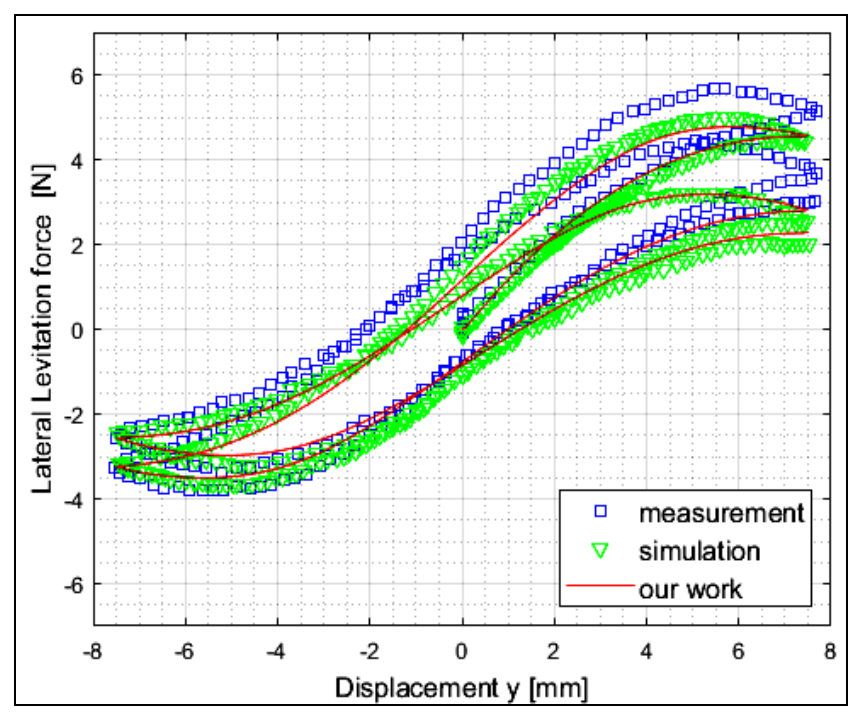


Fig 2: In our validation, vertical and lateral levitation forces depending on displacements, respectively. (a): Vertical levitation force, (b):

Lateral levitation force

The differences between our results and reference data are shown in table 2.

Displacement sequence points, (x, y, z)Levitation forces, N (0, 0, 5)(0, 7.5, 5)(0, -7.5, 5)(0, 7.5, 5)(0, -7.5, 5)(0, 7.5, 5)measurement 42.93 29.52 28.49 27.72 27.46 27.07 simulation 42.93 29.26 27.72 26.95 26.43 26.17 Vertical 27.22 our work 43.47 29.05 26.35 25.66 25.35 difference -0.54 0.21 0.5 0.6 0.77 0.82 measurement 0.35 5.05 -3.19 3.78 -2.56 3.03 simulation 0.039 4.42 -3.15 2.52 -2.52 2.01 Lateral our work 0.011 4.56 -3.24 2.81 -2.57 2.29 difference 0.028 -0.14 0.09 -0.29 0.05 -0.28

Table 2. The force differences between our results and reference data

The differences in table 2 are ones between our results and the previous experiments. As shown in table 2, the difference between our results and the ones of the previous experiments is relatively small in the first moving stage, but tends to increase gradually towards the last stage. However, our simulation time was 43255 s, much shorter than the previous simulation time of 392529 s [13]. We used a personal computer to perform the simulations in our article that has an Intel(R) i7-8750H, 2.20GHz, processor with 16 GB of random access memory.

3. Lateral Levitation Force in TSL-SMB

It had been simulated TSL-SMB in 2D axisymmetric system in ^[18], so that any lateral levitation force was not calculated. In this section, we consider the lateral levitation force

depending on the lateral displacements.

3.1. Comparing 2D axisymmetric H, H- ϕ formulation and 3D H- ϕ formulation in TSL-SMB

Again, the accuracy of our modeling is confirmed by comparing 2D axisymmetric H formulation, 2D axisymmetric H- ϕ formulation and 3D H- ϕ formulation in TSL-SMB. Firstly, the simulation with 2D axisymmetric H formulation was already presented in our article of Ref. 20. Secondly, the simulation with 2D axisymmetric H- ϕ formulation was performed to reflect the field cooling state as well as H-formulation. Thirdly, the simulation with 3D H- ϕ formulation was also performed to reflect the field cooling state. In all cases, the maximum displacement is 2.5 mm. The geometric parameters in figure 3 (a) are shown in table 3.

Table 3.geometric parameters on TSL-SMB

Symbol	Definition	Outer diameter × Inner diameter × Height, mm
HTS	Ring-type HTS bulk	90×50×20
PM_Inner	Inner PM on the ring-type HTS bulk	40×20×10
PM_Top	Top PM on the ring-type HTS bulk	80×60×10
PM_Bottom	Bottom PM on the ring-type HTS bulk	80×60×10

The modeling parameters are same as ones in table 1, but remanent flux density of PMs is 1.18 T. In figure 3 (b), the curve with blue color denotes the case of 2D axisymmetric H-formulation, the curve with green color denotes the case of 2D axisymmetric H- ϕ formulation, the curve with red

color denotes the case of 3D H- ϕ formulation. As shown in figure 3, the blue curve coincide with the green curve very good. In considering the red curve, the maximum vertical levitation force equals to one of the other curves, but the hysteresis loop is slightly different from the other ones.

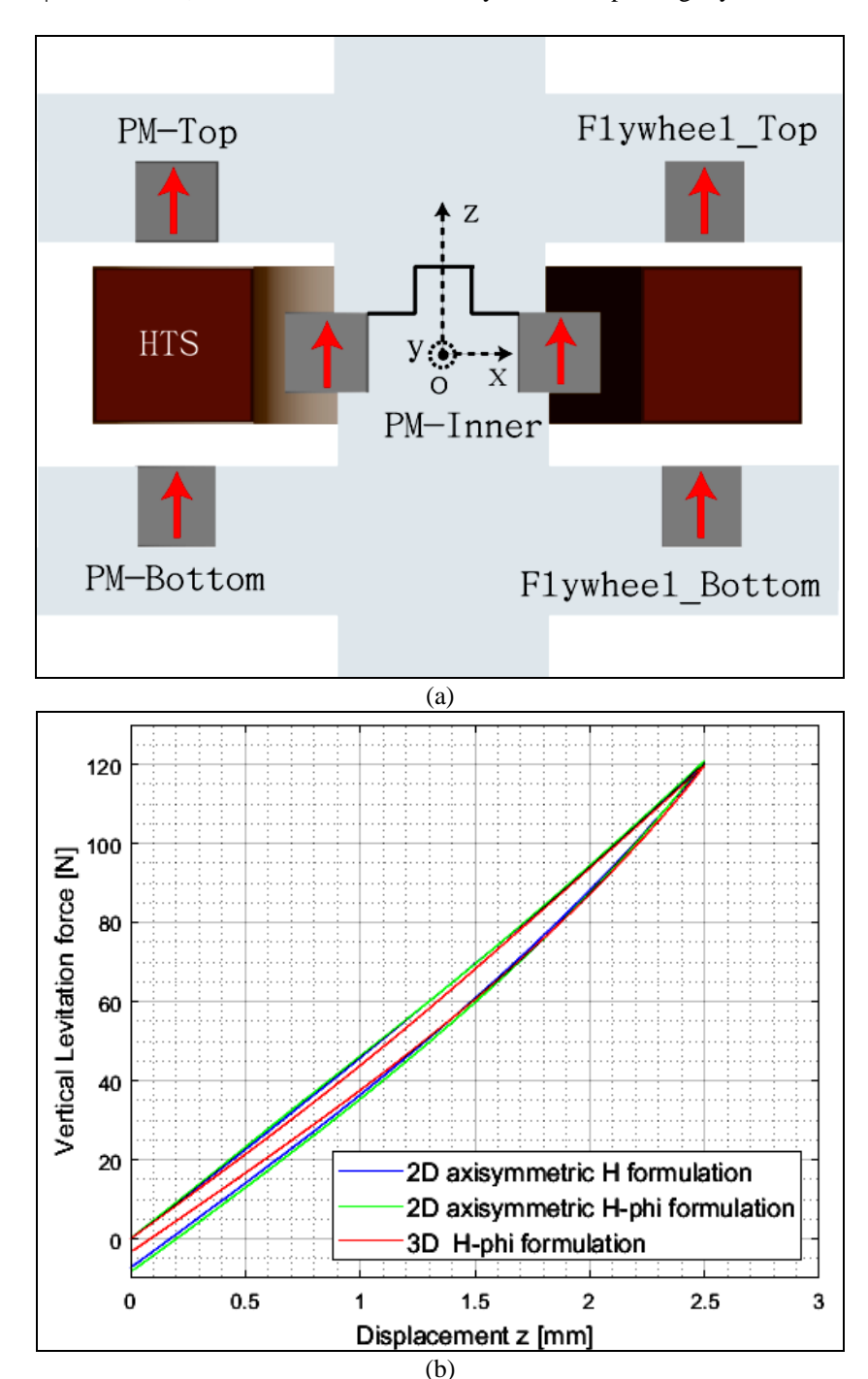


Fig 3: Schematic of TSL-SMB and comparing curve, (a): Schematic of TSL-SMB, (b): comparing curve between 2D axisymmetric H formulation, 2D axisymmetric H-φ formulation and 3D H-φ formulation

In 2D axisymmetric and 3D H- ϕ formulation, the mesh were discretized by the free triangular with maximum size of 1mm in HTS and PMs domain and free tetrahedral with maximum size of 2.5 mm on boundary of HTS and PMs, respectively. The mesh generated is presented in detail in

figure 4. And then, half volume of TSL-SMB is only considered, since it is enough to predict the vertical and lateral levitation force in 3D. The simulation times are 8500 s, 1650 s and 6720 s for 2D axisymmetric H, H- ϕ formulation and 3D H- ϕ formulation, respectively.

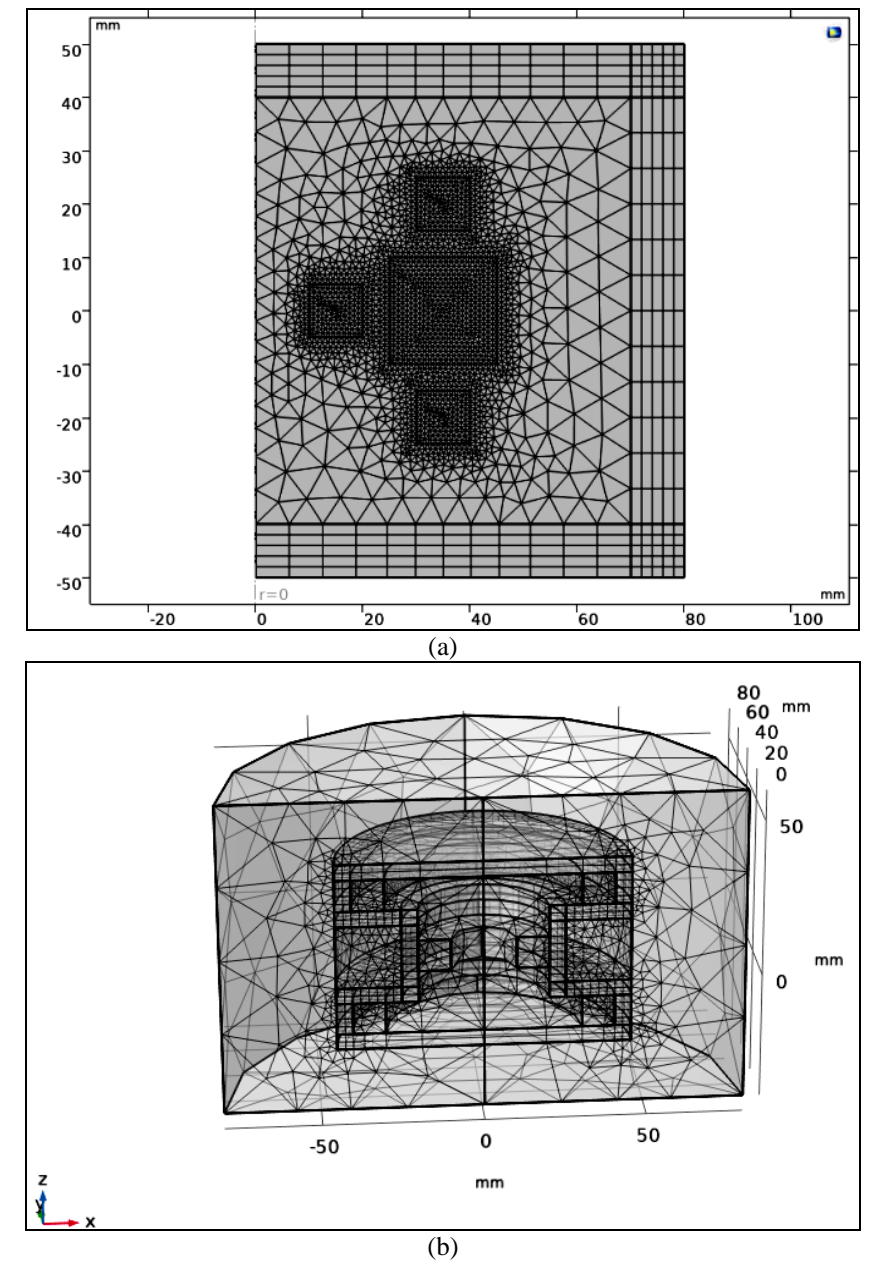


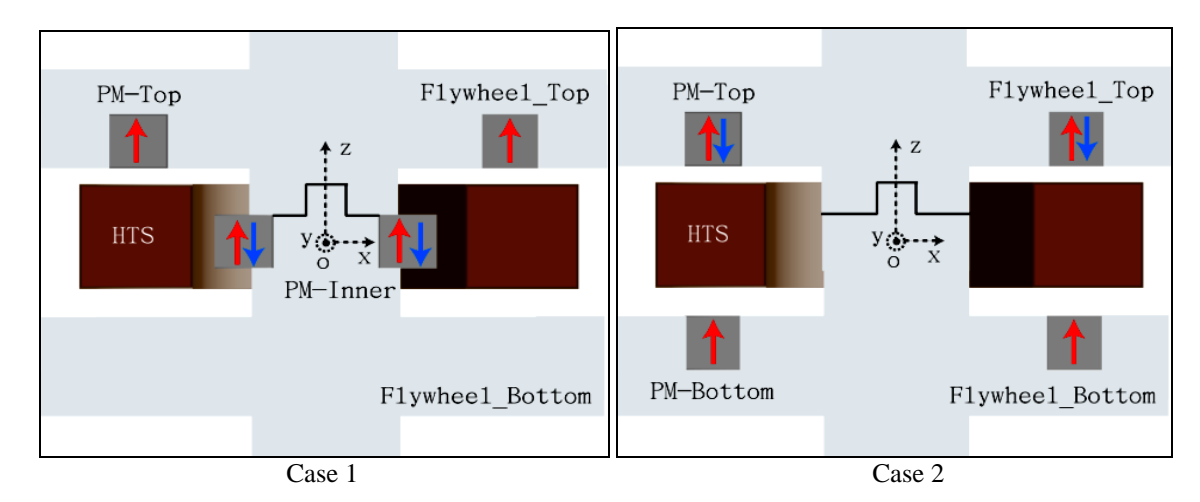
Fig 4: The meshes for 2D axisymmetric and 3D H-φ formulation, (a): 2D axisymmetric, (b):3D

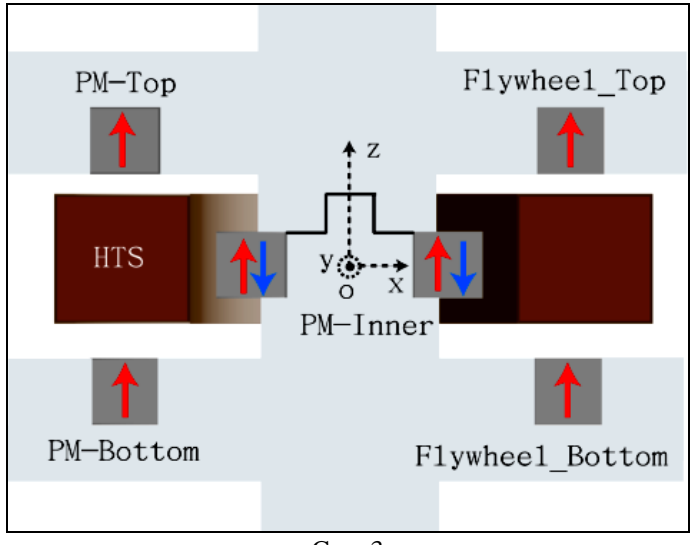
Based on the above verification, we predict the lateral forces according to magnetization arrangements of PMs in the TSL-SMB.

3.2. Vertical and lateral force with lateral displacements

in TSL-SMB

We calculate the vertical and lateral forces with lateral displacements in cases of magnetization arrangements, which are drew in figure 5.





Case 3

Fig 5: Magnetization arrangements in TSL-SMB

One assumes that the red arrow arrangements are attractive arrangements and the blue arrow arrangements are repulsive arrangements. In addition, if one assumes that the original points of flywheel rotor (i.e., object fixed the PMs) and flywheel stator (i.e., HTS) are coincided with the original point in coordinates, the moving sequences of flywheel rotor are as following:

 $\{(0, 0, 0), (0, 0, -2.5), (2, 0, -2.5), (-2, 0, -2.5), (0, 0, -2.5)\}$

when the moving speed is 1mm/s in all cases. Table 4 shows the simulation results for each case. As shown in table 4, the vertical force and the lateral ones in case 3 are the largest, and differences of the vertical levitation forces between 2th point (0, 0, - 2.5) and 5th point (0, 0, -2.5) are approximately 10 N. This shows that Case 3 is more favorable for TSL-SMB. However, it also shows that the lateral movement (i.e., vibration) is unfavorable in SMB systems.

Levitation force, N		Coordinate points				
		(0, 0, -2.5)	(2, 0, -2.5)	(-2, 0, -2.5)	(0, 0, -2.5)	
Case1	Attractive	Vertical	101.47	95.73	98.88	89.64
		Lateral	0.01	23.54	-26.62	1.12
	Repulsive	Vertical	75.17	71.76	73.72	64.65
		Lateral	0.19	22.82	-25.58	1.29
Case2	Attractive	Vertical	80.16	74.89	75.78	69.87
		Lateral	0.33	19.47	-21.03	1.23
	Repulsive	Vertical	85.05	79.00	80.42	74.49
		Lateral	0.35	17.9	-19.28	1.22
Case3	Attractive	Vertical	119.27	112.15	114.97	107.05
		Lateral	-0.05	30.51	-34.08	0.94
	Repulsive	Vertical	76.86	72.47	73.94	66.69
		Lateral	0.19	28.10	-31.04	1.37

Table 4:. Simulation results on each case

Figure 6 shows the vertical and lateral levitation forces depending on x-axis direction displacement. The red and the blue curves denote the case of the attractive magnetization arrangement, the red dash-dotted and the blue dash-dotted curves denote the case of the repulsive magnetization arrangement, respectively. In addition, abbreviations (i.e., VFA, VFR, LFA and LFR) mean the vertical levitation force of attractive arrangement, the vertical levitation force of repulsive arrangement, the lateral levitation force of

attractive arrangement and the lateral levitation force of repulsive arrangement, respectively. From the table 3 and figure 6, it can be seen that the vertical levitation forces for the attractive arrangement in Case 1 and Case 3 are larger than ones for the repulsive arrangement, and ones for the attractive arrangement in Case 2 is smaller than ones for the repulsive arrangement. The absolute values of the lateral levitation forces for the attractive arrangements are larger than ones for the repulsive arrangements in all cases.

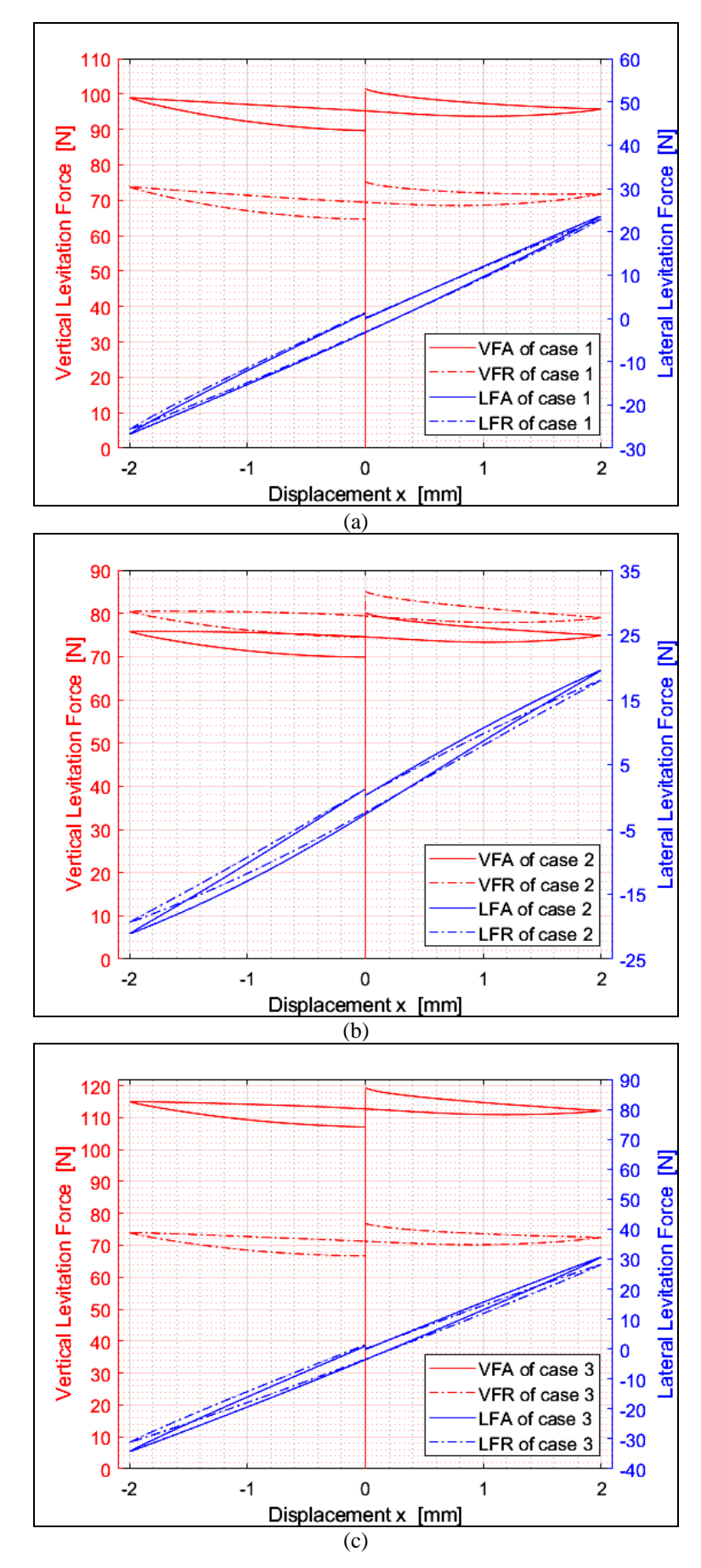


Fig 6: Vertical levitation force and lateral levitation force depending on x direction displacement. (a): Case 1, (b): Case 2, (c): Case 3

4. Lateral Levitation Force in TSL-SMB with ring-type PMs of opposite polarization

In this section, we predict the lateral levitation force of TSL-

SMB with ring-type PMs of opposite polarization. In figure 7, geometric parameters of PM_ Top and PM_ Bottom are $90{\times}50{\times}10$, respectively. In addition, parameter, r_t , has

selected three values such as 32.5 mm, 35mm, 37.5 mm and 40 mm. Table 5 shows the vertical levitation forces and lateral ones for different values of parameter, r_t. In table 5, the maximum value of vertical levitation force, 170.12 N, is

good agreement with ones of [17, 22], 170.14 N. The differences between the vertical levitation forces of 2^{th} point (0, 0, -2.5) and 5^{th} point (0, 0, -2.5) are approximately 30 N.

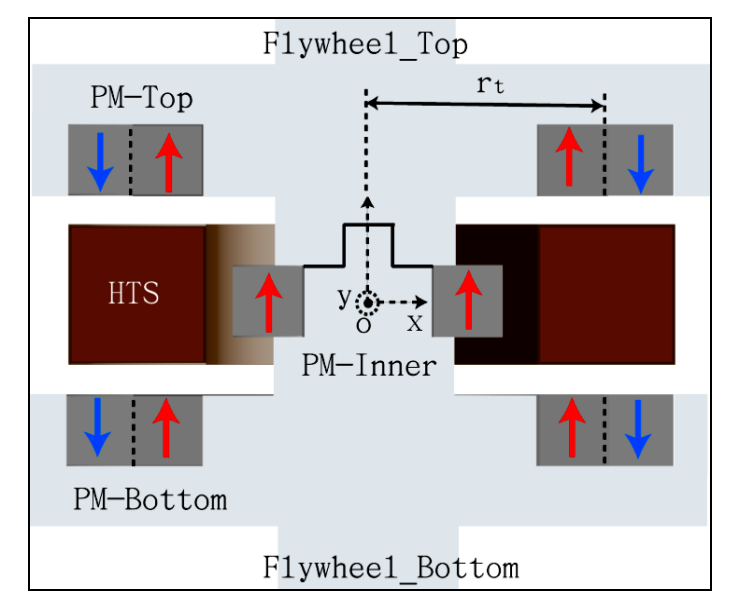


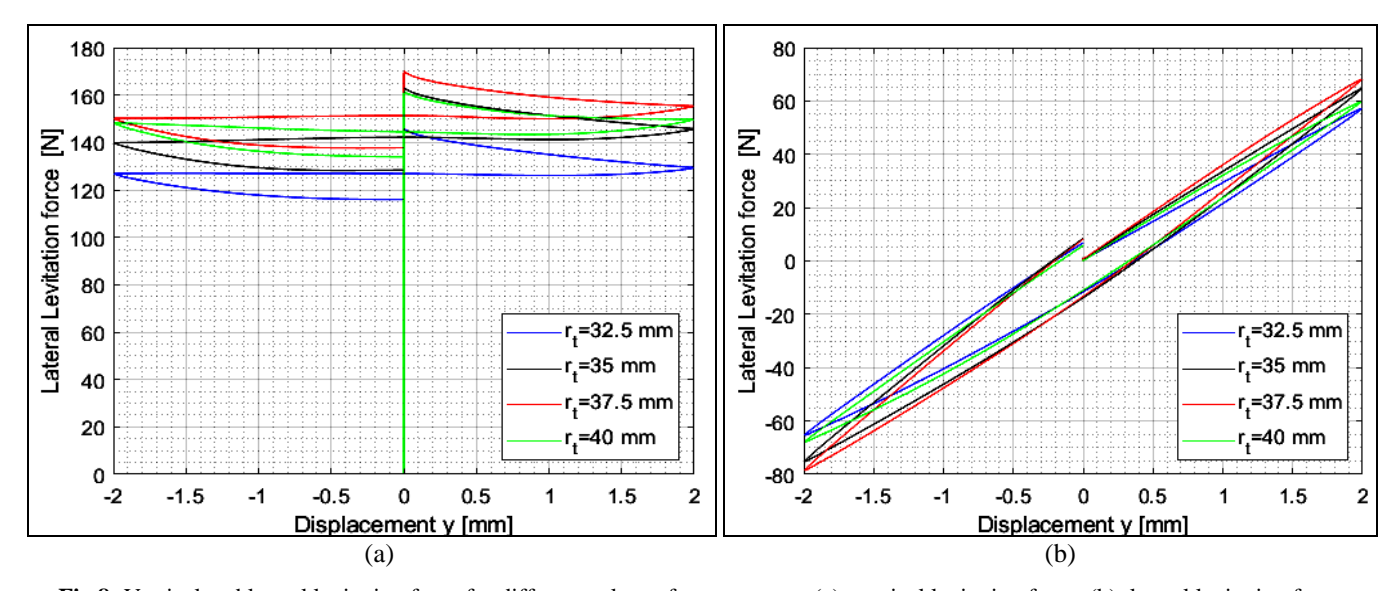
Fig 7: Schematic on TSL-SMB with ring-type PMs of the opposite polarization

radina mm	Levitation force, N	Coordinate points			
radius, mm		(0, 0, -2.5)	(0, 2, -2.5)	(0, -2, -2.5)	(0, 0, -2.5)
r _t =32.5	vertical	145.80	129.29	126.73	115.96
	lateral	0.52	57.08	-65.21	6.8
r _t =35	vertical	163.22	145.68	139.77	128.38
	lateral	0.95	64.55	-75.06	8.41
r _t =37.5	vertical	170.12	155.31	150.07	137.79
	lateral	0.92	68.07	-78.40	8.23
r _t =40	vertical	161.58	149.65	148.14	133.93
	lateral	0.39	59.79	-67.78	5.81

Table 5: Vertical and lateral levitation forces for different values of parameter, rt

Figure 8 shows the vertical levitation force and lateral ones for different values of parameter, r_t . As shown in figure 8, not only the vertical levitation force but also the lateral

levitation forces are the largest value in case of parameter, r_t =37.5 mm.



 $\textbf{Fig 8:} \ \ \text{Vertical and lateral levitation force for different values of parameter, } r_t, (a): \ \text{vertical levitation force, } (b); \ \text{lateral levitation force.}$

5. Results and Discussion

To examine the accuracy of simulation in TSL-SMB by 3D

H- ϕ formulation, it is compared with the simulation by H and H- ϕ formulation in 2D axisymmetric system, while the

simulation was performed in field cooling state. Here, the maximum vertical levitation force is approximately 120 N, which is in good agreement, and the hysteresis loop has a slight difference. To calculate the lateral levitation force, the vertical and lateral displacements were applied. In 3D system, the maximum vertical levitation force is 119.27 N at first sequence point (0, 0, -2.5), while the maximum lateral levitation force is 34.08 N at third sequence point (0, -2, -2.5). In TSL-SMB with ring-type PMs of opposite polarization, the former is 170.12 N, and the latter is 78.4 N. As the results, the vertical levitation force increased by 142.6% and the lateral levitation force by 230%. From the above-mentioned research results, we confirmed that TSL-SMB with ring-type PMs of opposite polarization is superior.

6. Conclusion

In this paper, the TSL-SMB is considered in 3D simulation, so that we have predicted the vertical and lateral levitation force with the lateral displacement. Firstly, we have performed a simulation verification of a single levitation system by the H- ϕ formulation, where a very good agreement with previous studies has been obtained. The simulation time was reduced by one third as comparing with the results of previous studies. The validation in TSL-SMB was also performed to obtain very good agreement in levitation force versus z-axis displacement. We applied the H-φ formulation by in COMSOL Multiphysics, so that PMs with complex scheme were flexibly modeled. By simulating the lateral levitation force in TSL-SMB, TSL-SMB with ring-type PMs of opposite polarization is also superior in the lateral force side. We calculated the basis of the design and operational stability of this bearing, which will contribute to the development of superconducting magnetic bearings with improved performance.

References

- Mukoyama S, et al. Development of superconducting magnetic bearing for 300 kW flywheel energy storage system. IEEE Trans Appl Supercond. 2017;27:3600804-12.
- 2. Gayathri NS, *et al.* Smoothing of wind power using flywheel energy storage system. IET Renew Power Gener. 2017;11:289-98.
- 3. Li J, *et al.* Research on improving power quality of wind power system based on the flywheel energy storage system. In: China International Conference on Electricity Distribution (CICED 2016); 2016. p.10-13.
- 4. Qiu Y, *et al.* Suppression of low-frequency vibration for rotor-bearing system of flywheel energy storage system. Mech Syst Signal Process. 2019;121:496-508.
- 5. Ichihara T, *et al.* Application of superconducting magnetic bearings to a 10 kWh-class flywheel energy storage system. IEEE Trans Appl Supercond. 2005;15:2245-8.
- Werfel FN, et al. A compact HTS 5 kWh/250 kW flywheel energy storage system. IEEE Trans Appl Supercond. 2007;17:2138-41.
- 7. Chen SL, *et al.* A new 3D levitation force measuring device for REBCO bulk superconductors. Physica C. 2014;496:39-43.
- 8. Sun RX, *et al.* Thickness dependence of the levitation performance of double-layer high-temperature superconductor bulks above a magnetic rail. Physica C.

- 2014:505:80-4.
- 9. Zhang XY, *et al.* Three-dimensional measurements of forces between magnet and superconductor in a levitation system. Physica C. 2007;467:125-9.
- 10. Espenhahn T, *et al.* Influence of the magnet aspect ratio on the dynamic stiffness of a rotating superconducting magnetic bearing. J Phys D. 2019;53:3-9.
- 11. Olabi AG, Wilberforce T, Abdelkareem MA, Ramadan M. Critical review of flywheel energy storage system. Energies. 2021;14:2159-72.
- 12. Sass F, Sotelo GG, Junior RA, Sirois F. H-formulation for simulating levitation forces acting on HTS bulks and stacks of 2G coated conductors. Supercond Sci Technol. 2015;28:125012-20.
- 13. Quéval L, Liu K, Yang W, Zermeño VM, Ma G. Superconducting magnetic bearings simulation using an H-formulation finite element model. Supercond Sci Technol. 2018;31:084001-12.
- 14. Ai L, Zhang G, Li W, Liu G, Liu Q. Optimization of radial-type superconducting magnetic bearing using the Taguchi method. Physica C. 2018;550:57-64.
- 15. Quéval L, *et al.* Optimization of the superconducting linear magnetic bearing of a maglev vehicle. IEEE Trans Appl Supercond. 2016;26:3601905-12.
- Grilli F, Morandi A, Silvestri FD, Brambilla R. Dynamic modeling of levitation of a superconducting bulk by coupled H-magnetic field and arbitrary Lagrangian-Eulerian formulations. Supercond Sci Technol. 2018;31:125003-15.
- 17. Jo JH, Ryu YG, Cho Y. Simulation on modified multisurface levitation structure of superconducting magnetic bearing for flywheel energy storage system by H-formulation and Taguchi method. Physica C. 2023;613:1354305-13.
- 18. Ma GT, *et al.* 3-D modeling of high-Tc superconductor for magnetic levitation/suspension application—Part II: validation with experiment. IEEE Trans Appl Supercond. 2010;20:2228-34.
- 19. Pratap S, *et al.* 3-D transient modeling of bulk high-temperature superconducting material in passive magnetic bearing applications. IEEE Trans Appl Supercond. 2015;25:5203910-8.
- Arsenault A, Sirois F, Grilli F. Implementation of the H-φ formulation in COMSOL Multiphysics for simulating the magnetization of bulk superconductors and comparison with the H-formulation. IEEE Trans Appl Supercond. 2021;31:6800111-20.
- 21. Li W, Wang D, Peng S, Deng Z. Optimizing superconducting magnetic bearing of HTS flywheel systems based on 3D H-φ formulation. Cryogenics. 2024;140:103849-58.
- 22. Yıldız AS, Sivrioglu S. Superconducting levitation analysis of a flywheel system using H-formulation. Physica C. 2019;561:64-70.